Contents lists available at NCBI

The American Journal of Science and Medical Research

Journal homepage: https://ajsmrjournal.com/

Research Article

Structure-Based Discovery of High-Affinity Inhibitors Targeting the Attachment Glycoprotein (NiV-G) of Nipah Virus

Madhav Morla[1], Bhavani Encharla[2], Estari Mamidala[3]

[1]Department of Biochemistry, Kakatiya University, Warangal-506009 TG, India.
[1]Department of Microbiology, SRR Government Arts and Science College, Karimnagar, Telangana, India-505001.
*[3]Department of Zoology, Kakatiya University, Warangal-506009 TG, India

[1] Email id: madhavmorla29@gmail.com; https://orcid.org/0009-0002-0346-898X

[2] Email id: incharlabhavani@gmail.com; https://orcid.org/0009-0003-7268-7112

*Corresponding author:
Email id: drestari@kakatiya.ac.in;
*https://orcid.org/0000-0002-7874-6019

https://dx.doi.org/10.5281/zenodo.21403505

Received: 4 June 2026
Revised: 09 July 2026
Published: 17 July 2026

ISSN: 2377-6196
Published by AIRA

Keywords: *Nipah virus, NiV-G, fusion protein, molecular docking*

ABSTRACT

Nipah virus (NiV) is a highly lethal emerging pathogen with no approved antiviral therapies, posing a significant global health threat. Viral entry is mediated by the attachment glycoprotein G (NiV-G) and the fusion protein (F), which initiates infection through receptor binding, making it a critical therapeutic target. Targeting NiV-G therefore represents an attractive strategy to block infection at its earliest stage. In the present study, a comprehensive in silico approach was employed to identify potential inhibitors of NiV-G. the top hit (PubChem ID: 134220125) achieved a docking score of −10.69 kcal·mol^{-1} (Ki ≈ 14.6 nM), surpassing the reference Acrivastine (PubChem: 5284514; −10.07 kcal·mol^{-1}, Ki ≈ 41.4 nM). Binding analyses indicate that high-affinity ligands engage a complementary mix of hydrogen bonds and extensive hydrophobic/van der Waals contacts within the receptor-binding groove. These results identify several nanomolar-range NiV-G binders as promising starting points for medicinal chemistry optimization and experimental validation. Further evaluation using molecular dynamics simulations and in vitro assays is recommended to confirm binding stability, target engagement, and antiviral efficacy. Additionally, optimizing these scaffolds could overcome the blood-brain barrier, which is essential for treating NiV-induced fatal encephalitis. Given the high case fatality rate and epidemic potential of Henipaviruses, translating these computational breakthroughs into viable preclinical candidates represents a critical step forward in establishing a robust frontline defense against emerging zoonotic threats.

1. Introduction

Nipah virus (NiV) is an emerging and highly pathogenic zoonotic virus belonging to the family Paramyxoviridae and naturally harbored by Pteropus fruit bats, which serve as the primary reservoir and facilitate zoonotic transmission to humans and domestic animals (Yang & Kar, 2023). The Nipah virus was first recognized during a substantial 1998 outbreak in Malaysia that primarily involved pig farmers. Since then, NiV has reappeared in multiple outbreaks throughout South and Southeast Asia, demonstrating its ability to spread regionally and cross species barriers. Human infections typically produce severe clinical illness, and outbreaks are often marked by high case-fatality rates (Faus-Cotino et al., 2024)(LEE, 2007). Nipah virus enters host cells through the coordinated action of two surface glycoproteins: the attachment protein (G) and the fusion protein (F). The G protein binds to receptors on the host cell surface, while the F protein mediates membrane fusion between the virus and the host cell. NiV has triggered outbreaks across multiple countries, with documented mortality rates between 40% - 70%. Infected individuals frequently develop acute respiratory disease alongside severe neurological complications, notably fatal encephalitis (World Health Organization, 2026) (LEE, 2007; Kumar et al.., 2020).

Nipah virus (NiV) induces direct cell-to-cell fusion within the host, leading to the formation of multinucleated giant cells known as syncytia. This mechanism enables efficient viral dissemination even in the absence of conventional viral budding, thereby substantially enhancing infectivity. The incubation period typically ranges from 4 to 14 days. Although NiV predominantly targets the central nervous system, outbreaks caused by strains circulating in Bangladesh have demonstrated pronounced respiratory involvement. Furthermore, NiV exhibits a high mutation rate and is associated with persistently elevated mortality, with no approved specific antiviral therapy currently available (Singh et al., 2019) (World Health Organization, 2026; Porika et al., 2014).

In the present study, we therefore focus on the G glycoprotein (NiV-G) as a strategic target for structure-based drug discovery. Inhibition of NiV-G has the potential to block viral entry at its initiation, thereby suppressing downstream replication and spread. Owing to its surface accessibility, functional indispensability, and defined receptor-binding interface, NiV-G represents a highly promising target for the development of antiviral therapeutics and vaccine candidates. In the absence of effective therapeutic options, there is a critical need for innovative strategies in antiviral drug discovery against Nipah virus. The present study aims to identify potential inhibitors targeting the NiV-G using a comprehensive in silico approach. This workflow integrates virtual screening, molecular docking, and molecular dynamics simulations to systematically evaluate candidate compounds. Molecular docking enables detailed characterization of ligand–protein binding modes and key interaction patterns within the NiV-G active site, while molecular dynamics simulations further assess the stability of these complexes under physiological conditions. Collectively, the application of these advanced computational techniques provides a robust framework to support antiviral drug discovery and contributes to broader public health efforts aimed at mitigating future Nipah virus outbreaks (Randhawa et al., 2022; Mamidala et al., 2020).

2. Materials & Methods

2.1. Selection and Preparation of Target Macromolecule

The target macromolecule, NIPAH VIRUS GLYCOPROTEIN (NiV-G), was selected based on entry of Nipah virus and plays key role in antiviral drug discovery. The three-dimensional crystal structure of Nipah Virus Glycoprotein (PDB:2VSM) was retrieved from RCSB-Protein Data Bank (https://www.rcsb.org). The selection of NIPAH VIRUS GLYCOPROTEIN (NiV-G) was justified due to its high resolution (1.80 Å) X-ray crystallographic structure in complex with Erphri-B2, NAG and IPA (Bowden et al., 2008).
To prepare the target protein for molecular docking, the different steps where we performed using AutoDock 4.2 Molecular Graphics Laboratory (MGL) Tools version 1.5.7. steps include ligands, heteroatoms and water molecules are removed. Hydrogens added at polar ends, Kollman united atom charges and Gasteiger charges were assigned.

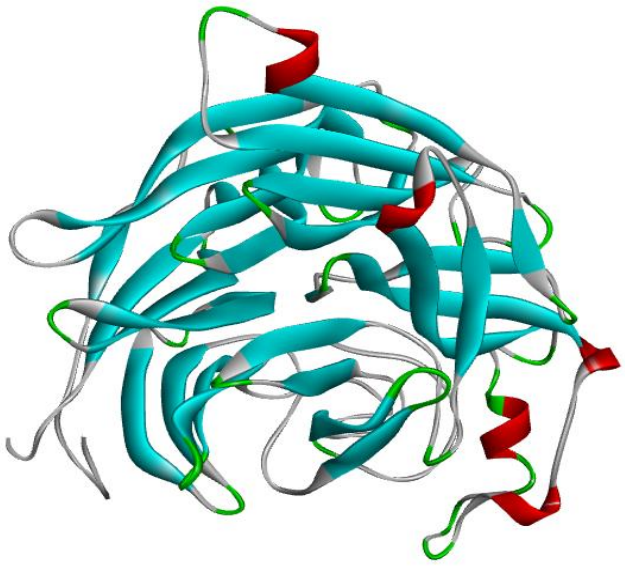

Figure-1. 3D crystal structure of Nipah Virus Glycoprotein (PDB:2VSM)

To ensure stable starting conformation, the protein was subjected to energy minimization, effectively eliminating steric hindrance and optimizing structural geometry. Lastly, prepared protein was saved in PDBQT format (Morris et al., 2009; Lunavath et al., 2013; Poojari et al., 2014).

2.2. Selection And Preparation of Ligands and Virtual Screening

Ligand selection and preparation are very pivotal steps in molecular docking stimulation studies. As they determine the binding affinity, potentially target the NiV-G inhibits viral entry. The virtual screening was employed to identify the antiviral agents by inhibiting by NiV-G from Pharmit search engine (https://pharmit.csb.pitt.edu) and ligands were retrieved from the PubChem database (https://pubchem.ncbi.nlm.nih.gov). the selection of ligands is Critical for Pharmacophore modelling. Pharmacophoric features, including hydrogen-bond acceptors and donors, aromatic ring systems, and molecular shape descriptors, were defined to guide the identification of potential inhibitors. To ensure drug-like properties, stringent filtering criteria were applied: molecular weight ≤ 500 g/mol, rotatable bonds ≤ 10, lipophilicity (LogP) ≤ 10, polar surface area ≤ 150 Å², hydrogen-bond donors ≤ 5, and hydrogen-bond acceptors ≤ 10 (Koes, 2018). The PubChem database was selected as the screening library due to its extensive and diverse chemical coverage. Following optimization of these parameters, the pharmacophore-based search was executed, yielding a refined set of compounds that satisfied all predefined criteria. (National Center for Biotechnology Information, n.d.).

After Pharmacophore modelling, the selected compounds PubChem5284514 (Acrivastine) PubChem70233457, PubChem134220125, PubChem448238, PubChem110153556, PubChem12937927 and PubChem126090111. The selected compounds were retrieved from the PubChem database and converted into AutoDock-compatible file formats (PDB, PDBQT, and MOL) using Open Babel. Ligand preparation was performed using AutoDock 4.2, which involved the assignment of root atoms, definition of torsional flexibility and active rotatable bonds, followed

2.3. Molecular Docking Simulation Studies

The 2VSM (NiV-G) was subjected to molecular docking studies using AutoDock 4.2 tools. A blind docking approach was conducted with grid box (126×126×126 points centred in protein with a spacing of 0.397 Å. A grid box encompassing the entire protein was defined to ensure comprehensive coverage of potential ligand-binding sites. Grid parameters were saved in the grid parameter file (GPF) format to guarantee consistency across runs. Molecular docking was carried out using the Lamarckian Genetic Algorithm (LGA) implemented in AutoDock 4.2 with the following protocol parameters: 10 trial runs, population size = 150, maximum energy evaluations = 2,500,000, maximum generations = 27,000, mutation rate = 0.02, crossover rate = 0.8, and elitism = 1. Docking parameter files (DPF) were generated and AutoGrid and AutoDock were executed to produce GLG and DLG output files, which contain results from all trial runs including binding energies, inhibition constants, component energy terms, and hydrogen-bonding information. Protein–ligand complexes were analyzed and ranked by lowest binding energy; top-scoring poses were saved in PDB format and used for subsequent protein–ligand interaction analyses (Lohning et al., 2017; Namthabad et al., 2014; Swapna et al., 2024).

3. Results

3.1 Molecular Docking Results

The molecular docking stimulation study evaluated seven antiviral compounds against Nipah virus, including Acrivastine. The results reveal the significant variation in binding affinity and protein-ligand interaction patterns.

NiV-G Binding Interaction With Acrivastine :

This ligand exhibited a binding energy of −10.07 kcal/mol and an inhibition constant of 41.37 nM. 2 hydrogen bonds were formed with ILE514, CYS565. And the hydrophobic interactions with residues such as ASP515, ile572, LEU513, LEU448, SER447, GLU226, PHE566, GLY227, VAL255, ASP225, MET224, ASN564, ILE356, TYR445, ILE444, GLY355, ASP446, PHE512.

NiV-G Binding Interaction With Pubchem70233457:

This ligand demonstrated a binding energy of −9.12kcal/mol and an inhibition constant of 207.95nM. 3 hydrogen bonds were formed with LEU567, ASP446, ASN546. And other hydrophobic interactions at GLU226, ASP225, TYR445, PHE512, CYS565, MET224, VAL255, TYR228, PHE566, GLY227. LEU568.

NiV-G Binding Interaction With Pubchem134220125

This ligand demonstrated a binding energy of −10.69kcal/mol and an inhibition constant of 14.57nM. 2 hydrogen bonds were formed with ASP446, ASP225. And other hydrophobic interactions at MET224, TYR228, GLY227, VAL255, PHE566, CYS565, LYS357, LEU567, PHE512.

NiV-G binding interaction with pubchem448238

This ligand demonstrated a binding energy of −8.15kcal/mol and an inhibition constant of 1.06uM. 3 hydrogen bonds were formed with LEU567, VAL255(2). And other hydrophobic interactions at MET224, PHE566, ASN564, ASP225, CYS565, ASP446, SER447, PHE512, LEU448, GLU226, LEU568, GLY227, LEU256.

NiV-G binding interaction with Pubchem110153556

This ligand demonstrated a binding energy of −9.59kcal/mol and an inhibition constant of 96.59nM. 2 hydrogen bonds were formed with ILE514, LEU448. And other hydrophobic interactions at ILE572, TRP573, PHE566, LEU567, HLU226. GLY227, GLY449, ASP225, SER225, SER447, ASP446, ASN564, LEU513, CYS565, MET224, PHE512.

NiV-G Binding Interaction with Pubchem12937927

This ligand demonstrated a binding energy of −7.41kcal/mol and an inhibition constant of 3.73uM. 5 hydrogen bonds were formed with ASN564, ASP446, CYS565. And other hydrophobic interactions a PHE566, MET224, PHE512, LEU448, ILE572, ILE514, LEU513, SER447, TYR445, LEU567, ASP225, GLU226, GLY227.

NiV-G binding interaction with pubchem126090111

This ligand demonstrated a binding energy of −9.59kcal/mol and an inhibition constant of 93.76NM. 2 hydrogen bonds were formed with LEU567, ASP446. And other hydrophobic interactions at LEU448, SER447, GLU226, MET224, GLY227, PHE566, ASN564, ASP225, TYR445, GLY355, ILE356, PHE512, CYS565, LEU513, ILE572, ILE514.

Table 1. Binding energy values, inhibition constant, H-bonds and other interactive bonds residues information of NiV-G with respective ligands

S. No	Compound name (ID)	Binding energy (δg) (kcal/mol)	Inhibition constant	No of h-bonds	H-bonds forming residues	Hydrophobic interaction
1	PubChem: 5284514; Acrivastine	-10.07 kcal/mol	41.37 nM	2	Ile514, Cys565	Asp515, Ile572, Leu513, Leu448, Ser447, Glu226, Phe566, Gly227, Val255, Asp225, Met224, Asn564, Ile356, Tyr445, Ile444, Gly355, Asp446, Phe512.
2	PubChem: 70233457	-9.12 kcal/mol	207.95nM	3	Leu567, Asp446, Asn546.	Glu226, Asp225, Tyr445, Phe512, Cys565, Met224, Val255, Tyr228, Phe566, Gly227. Leu568
3	PubChem: 134220125	-10.69 kcal/mol	14.57nM	2	Asp225, Asp446.	Met224, Tyr228, Gly227, Val255, Phe566, Cys565, Lys357, Leu567, Phe512
4	PubChem: 448238	-8.15 kcal/mol	1.06uM	3	Leu567, Val255(2)	Met224, Phe566, Asn564, Asp225, Cys565, Asp446, Ser447, Phe512, Leu448, Glu226, Leu568, Gly227, Leu256
5	PubChem: 110153556	-9.59 kcal/mol	96.56nM	2	Ile514, Leu448.	Ile572, Trp573, Phe566, Leu567, Hlu226. Gly227, Gly449, Asp225, Ser225, Ser447, Asp446, Asn564, Leu513, Cys565, Met224, Phe512.
6	PubChem: 12937927	-7.41 kcal/mol	3.73uM	5	Asn564, Asp446(2), Cys565(2).	Phe566, Met224, Phe512, Leu448, Ile572, Ile514, Leu513, Ser447, Tyr445, Leu567, Asp225, Glu226, Gly227
7	PubChem: 126090111	-9.59 kcal/mol	93.76nM	2	Leu567, Asp446.	Leu448, Ser447, Glu226, Met224, Gly227, Phe566, Asn564, Asp225, Tyr445, Gly355, Ile356, Phe512, Cys565, Leu513, Ile572, Ile514

Figure-2. Interaction analysis between NiV-G with Respective Compounds at the binding groove; NiV-G and compounds surface view of interactions, 3D & 2D interactions view of NiV-G and compounds

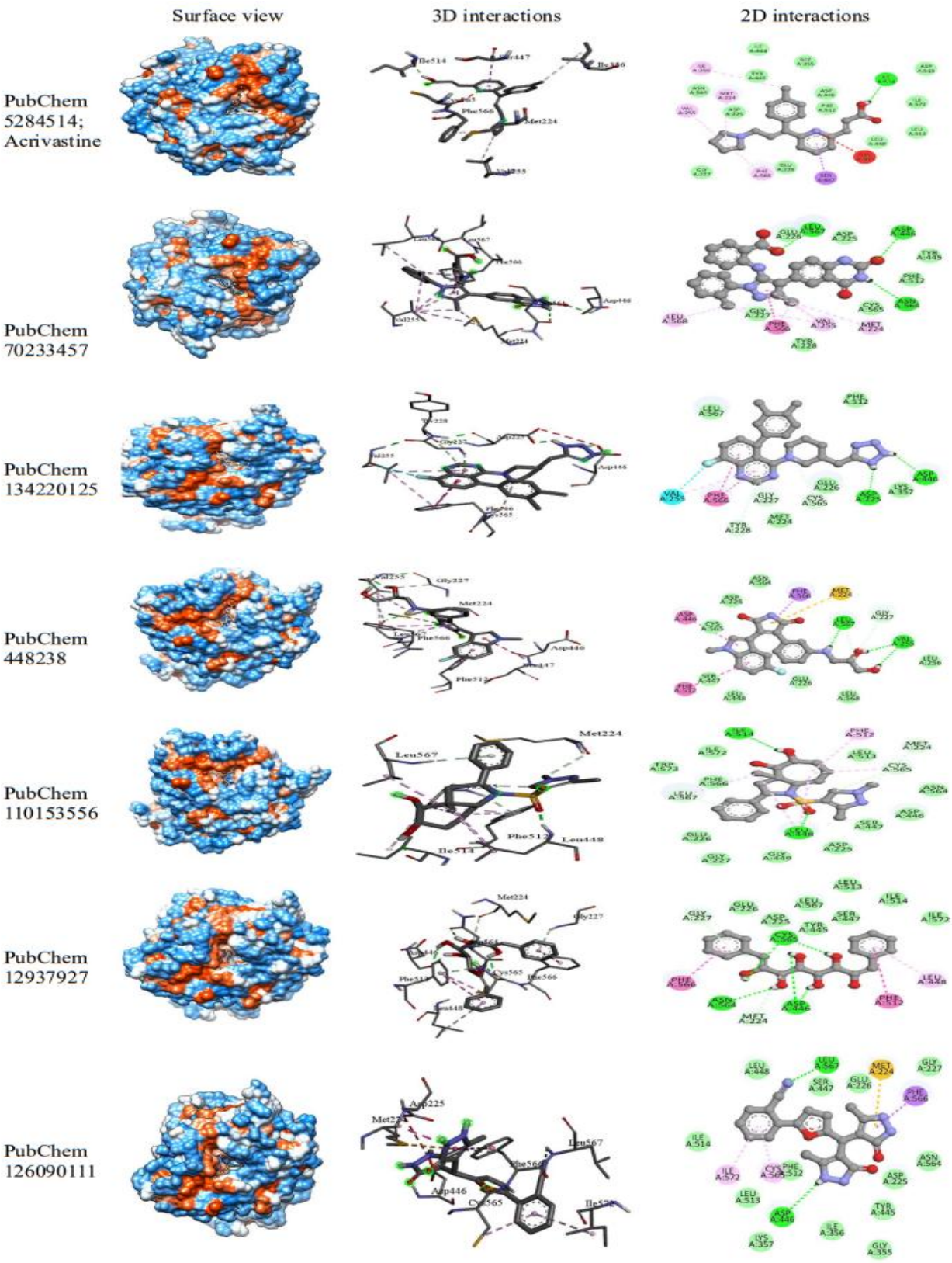

Analysis of molecular docking results

The molecular docking study evaluated seven ligands—consisting Acrivastine and six candidate compounds against the NiV-G binding site. These simulations, conducted using a blind docking approach and the Lamarckian Genetic Algorithm, revealed significant variations in binding affinities and interaction patterns among the tested compounds. The results highlight a diverse landscape of molecular recognition, with inhibition constants spanning from low nanomolar to micromolar ranges.

Binding Affinity and Inhibition Potential

Seven ligands were docked against the NiV-G, with Acrivastine used as the reference inhibitor. The docking scores ranged between −7.41 kcal/mol and −10.69 kcal/mol, corresponding to inhibition constants from the micromolar to low nanomolar range. Among these, PubChem ID: 134220125 stood out as the most potent candidate, recording a binding energy of −10.69 kcal/mol and an inhibition constant of 14.57 nM, which is markedly stronger than Acrivastine (−10.07 kcal/mol, Ki ≈ 41.37 nM). Other compounds, including PubChem IDs 110153556 and 126090111, also demonstrated nanomolar inhibition constants (≈ 93–96 nM), suggesting that they may serve as promising scaffolds for antiviral development.

Hydrogen Bonding and Residue Interactions

Hydrogen bonding played a central role in stabilizing ligand interactions within the NiV-G binding groove. Acrivastine formed two hydrogen bonds with ILE514 and CYS565, while the lead compound (PubChem 134220125) established two hydrogen bonds with ASP225 and ASP446, residues that are critical for receptor engagement. Interestingly, PubChem 12937927 formed five hydrogen bonds, yet its binding energy was weaker (−7.41 kcal/mol, Ki ≈ 3.73 μM). This observation reinforces that hydrogen bond count alone does not guarantee stronger affinity; the orientation and complementarity of these interactions are more decisive in determining stability.

Structural Insights and Binding Mode Analysis

Hydrophobic and van der Waals interactions provided additional stabilization across all ligand complexes. The lead compound (PubChem 134220125) engaged a broad non-polar network involving MET224, TYR228, GLY227, VAL255, PHE566, CYS565, LYS357, LEU567, and PHE512, ensuring strong occupancy of the binding cavity. In contrast, Acrivastine displayed a narrower hydrophobic profile, interacting with residues such as ASP515, LEU448, GLU226, PHE566, and TYR445, which explains its slightly weaker binding affinity compared to the lead compound.

Comparative Pharmacological Implications

The comparative docking analysis shows that several ligands achieved nanomolar inhibition constants, placing them within the range of next-generation antiviral agents. The superior binding affinity of PubChem 134220125 highlights its potential as a lead scaffold for further optimization. While Acrivastine remains a useful benchmark, multiple candidate ligands demonstrated stronger binding energies and more extensive interaction networks, supporting the rationale for structure-based drug discovery targeting NiV-G as a viable antiviral strategy.

4. Discussion

The molecular docking results shows how the antiviral agents are interacting with Nipah virus Glycoprotein. Compare to FDA approved Acrivastine drug, several compounds showing best binding strength. Particularly noteworthy is our lead compound's interactions with CYS565, ILE514, LEU567, ASP446, ASN564, ASP225, MET224, PHE566, ASP225, GLY355, TYR445 and other residues, and which corroborates the findings of Sangitha Ghimire et al (Adeniji et al., 2012), regarding this residue's crucial role in NiV G activity. we observed that compounds with more hydrogen bonds and stronger hydrophobic interactions compare to Acrivastine drug, such as our top-performing ligand, achieved superior binding energies. So, the results support the game changer in drug discovery via targeting NiV G highlighted in recent reviews.

This molecular docking study finds the antiviral compounds for effective NiV-G inhibitors. and listed compounds in table:1 are compared with Acrivastine drug. That compounds have similar features, that are similar protein-ligands interactions pharmacophore, low binding energy, inhibition constant (Table:1). In mentioned compounds Among them, compound PubChem ID: 134220125 Demonstrated the most potent binding energy of −10.69 kcal/mol, inhibition constant of 14.57 nM and 2 hydrogen bonds, outperforming the Acrivastine (−10.04 kcal/mol, 41.37 nM). And other compounds are also showing best hydrogen interactions with good binging energy indicating strong therapeutic antiviral compounds.

These findings have significant therapeutic implications, aligning with contemporary antiviral research. Our most potential antiviral compounds demonstrated inhibition at nanomolar range, comparable to next-generation antiviral agents to targets the Nipah Virus. Translating there in-silico results to clinical efficacy required to potential metabolic stability issues common to high-affinity compounds. Future work should incorporate the molecular dynamics approaches recommended to assess binding stability under physiological conditions. these findings of this study contribute to the growing body of evidence supporting structure-based design of Nipah-targeting based antiviral therapies, while highlighting the need for preclinical evaluation of compounds.(Morla Madhav & Mamidala Estari, 2025; Gujjeti et al., 2014; Gurrapu et al., 2017; Janakiramulu et al., 2025)

5. Conclusion

This study employed a structure-based molecular docking approach to identify potential inhibitors of the Nipah virus attachment glycoprotein (NiV-G), a key target for blocking viral entry. Several compounds demonstrated strong binding affinities, with some surpassing the reference drug Acrivastine. Among them, PubChem ID: 134220125 emerged as the most promising candidate, exhibiting the lowest binding energy and a nanomolar-range inhibition constant, indicating high inhibitory potential. Detailed interaction analysis revealed that effective binding is driven by a combination of hydrogen bonding and hydrophobic interactions with critical residues within the receptor-binding pocket, contributing to stability and specificity. These findings emphasize the importance of molecular complementarity in antiviral drug design. Although based on computational predictions, the results provide a solid foundation for further investigation. Future studies, including molecular dynamics simulations and experimental validation, are essential to confirm the stability, efficacy, and therapeutic potential of these compounds against Nipah virus infection.

Competing interests:

The authors declare that they have no competing interests

References

[1] Bowden, T. A., Aricescu, A. R., Gilbert, R. J. C., Grimes, J. M., Jones, E. Y., & Stuart, D. I. (2008). Structural basis of Nipah and Hendra virus attachment to their cell-surface receptor ephrin-B2. *Nature Structural & Molecular Biology*, *15*(6), 567–572. https://doi.org/10.1038/nsmb.1435

[2] Faus-Cotino, J., Reina, G., & Pueyo, J. (2024). Nipah Virus:

A Multidimensional Update. *Viruses*, *16*(2), 179. https://doi.org/10.3390/v16020179

[3] Koes, D. R. (2018). The Pharmit Backend: A Computer Systems Approach to Enabling Interactive Online Drug Discovery. *IBM Journal of Research and Development*, *62*(6), 1–6. https://doi.org/10.1147/jrd.2018.2883977

[4] LEE, B. (2007). Envelope–Receptor Interactions in Nipah Virus Pathobiology. *Annals of the New York Academy of Sciences*, *1102*(1), 51–65. https://doi.org/10.1196/annals.1408.004

[5] Lohning, A. E., Levonis, S. M., Williams-Noonan, B., & Schweiker, S. S. (2017). A Practical Guide to Molecular Docking and Homology Modelling for Medicinal Chemists. *Current Topics in Medicinal Chemistry*, *17*(18), 2023–2040. https://doi.org/10.2174/1568026617666170130110827

[6] Morla Madhav, & Mamidala Estari. (2025). In silico molecular docking studies for identify to potential androgen receptor blocking agents to treat prostate cancer. *RECENT TRENDS IN ANIMAL BIOTECHNOLOGY (RTAB-2024)*, 117–126. https://www.researchgate.net/publication/392172002

[7] Morris, G. M., Huey, R., Lindstrom, W., Sanner, M. F., Belew, R. K., Goodsell, D. S., & Olson, A. J. (2009). AutoDock4 and AutoDockTools4: Automated docking with selective receptor flexibility. *Journal of Computational Chemistry*, *30*(16), 2785–2791. https://doi.org/10.1002/jcc.21256

[8] National Center for Biotechnology Information. (n.d.). *PubChem Compound Summary for CID 5284514, Acrivastine*. Retrieved March 1, 2026, from https://pubchem.ncbi.nlm.nih.gov/compound/Acrivastine

[9] Randhawa, V., Pathania, S., & Kumar, M. (2022). Computational Identification of Potential Multitarget Inhibitors of Nipah Virus by Molecular Docking and Molecular Dynamics. *Microorganisms*, *10*(6), 1181. https://doi.org/10.3390/microorganisms10061181

[10] Sangita Ghimire, Sazzad Shahrear, Siddhesh Kishor Saigaonkar, & Laura K. Harris. (2022). Identification of Potential Inhibitors against Attachment Glycoprotein G of Nipah Virus using Comprehensive Drug Repurposing Approach. *International Journal of Biometrics and Bioinformatics (IJBB)*, *15*(1), 1–20. https://www.cscjournals.org/library/manuscriptinfo.php?mc=IJBB-268

[11] Singh, R. K., Dhama, K., Chakraborty, S., Tiwari, R., Natesan, S., Khandia, R., Munjal, A., Vora, K. S., Latheef, S. K., Karthik, K., Singh Malik, Y., Singh, R., Chaicumpa, W., & Mourya, D. T. (2019). Nipah virus: epidemiology, pathology, immunobiology and advances in diagnosis, vaccine designing and control strategies - a comprehensive review. *The Veterinary Quarterly*, *39*(1), 26–55. https://doi.org/10.1080/01652176.2019.1580827

[12] World Health Organization. (2026, January 29). *Nipah virus [Fact sheet]*. Https://Www.Who.Int/News-Room/Fact-Sheets/Detail/Nipah-Virus. https://www.who.int/news-room/fact-sheets/detail/nipah-virus

[13] Yang, S., & Kar, S. (2023). Are we ready to fight the Nipah virus pandemic? An overview of drug targets, current medications, and potential leads. *Structural Chemistry*, *34*(6), 2119–2137. https://doi.org/10.1007/s11224-023-02148-6.

[14] Gujjeti, R. P., Namthabad, S., & Mamidala, E. (2014). HIV-1 reverse transcriptase inhibitory activity of Aerva lanata plant extracts. *BMC Infectious Diseases*, *14*(Suppl 3), P12.

[15] Gurrapu, S., & Mamidala, E. (2017). In Vitro HIV-1 reverse transcriptase inhibition of andrographolide isolated from Andrographis paniculata. *European Journal of Biomedical*, *4*(12), 516-522.

[16] Janakiramulu, P., & Mamidala, E. (2025). Molecular Docking and dynamic simulation analysis of flavonoid derivatives as COX-2 inhibitors. *In Silico Pharmacology*, *13*(2), 59.

[17] Namthabad, S., & Mamidala, E. (2014). Molecular docking of HIV-1 protease using alkaloids from tinospora cordifolia. *Int J Res Appl*, *1*(1), 12-6.

[18] Swapna, K., Srujana, M., & Mamidala, E. (2024). Identification of steroidal cardenolides from *Calotropis procera* as novel HIV-1 PR inhibitors: A molecular docking & molecular dynamics simulation study. *The Indian journal of medical research*, *160*(1), 78.

[19] Lunavath, V., & Mamidala, E. (2013). Preliminary phytochemical screening and antibacterial studies of the leaves of Eclipta alba (L). *Int J Pharma Biosci*, *4*, 380-4.

[20] Kumar, M. P., Mamidala, E., Al-Ghanim, K., Al-Misned, F., Ahmed, Z., & Mahboob, S. (2020). Effects of D-Limonene on aldose reductase and protein glycation in diabetic rats. Journal of King Saud University-Science, 32(3), 1953-1958.

[21] Porika, R., Poojari, S., Lunavath, V., & Mamidala, E. (2014). Preliminary phytochemical investigation and TLC analysis of P. angulata fruit extract. Journal of Pharmacy and Biological Sciences, 9(2), 11-14.

[22] Kumar Thatipamula, R., Narsimha, S., Battula, K., Chary, V. R., Mamidala, E., & Reddy, N. V. (2017). Synthesis, anticancer and antibacterial evaluation of novel (isopropylidene) uridine-[1, 2, 3] triazole hybrids. Journal of Saudi Chemical Society, 21(7), 795-802.

[23] Poojari, S., Porika, R., & Mamidala, E. (2014). Phytochemical analysis and in vitro antidiabetic activities of Physalis angulata fruit extracts. *Natl. J. Integr. Res. Med*, *5*, 34-38.

[24] Mamidala, E., Davella, R., Gurrapu, S., & Shivakrishna, P. (2020). In silico identification of clinically approved medicines against the main protease of SARS-CoV-2, causative agent of covid-19. *arXiv preprint arXiv:2004.12055*.